Binding of bisubstrate analog promotes large structural changes in the unregulated catalytic trimer of aspartate transcarbamoylase: Implications for allosteric regulation

James A. Endrizzi*, Peter T. Beernink*†, Tom Alber, and H. K. Schachman‡

Department of Molecular and Cell Biology and Virus Laboratory, University of California, Berkeley, CA 94720-3206

Contributed by H. K. Schachman, February 29, 2000

A central problem in understanding enzyme regulation is to define the conformational states that account for allosteric changes in catalytic activity. For *Escherichia coli* aspartate transcarbamoylase (ATCase; EC 2.1.3.2) the active, relaxed (R state) holoenzyme is generally assumed to be represented by the crystal structure of the complex of the holoenzyme with the bisubstrate analog *N*-phosphonacetyl-L-aspartate (PALA). It is unclear, however, which conformational differences between the unliganded, inactive, taut (T state) holoenzyme and the PALA complex are attributable to localized effects of inhibitor binding as contrasted to the allosteric transition. To define the conformational changes in the isolated, nonallosteric C trimer resulting from the binding of PALA, we determined the 1.95-Å resolution crystal structure of the C trimer–PALA complex. In contrast to the free C trimer, the PALA-bound trimer exhibits approximate threefold symmetry. Conformational changes in the C trimer upon PALA binding include ordering of two active site loops and closure of the hinge relating the N- and C-terminal domains. The C trimer–PALA structure closely resembles the liganded C subunits in the PALA-bound holoenzyme. This similarity suggests that the pronounced hinge closure and other changes promoted by PALA binding to the holoenzyme are stabilized by ligand binding. Consequently, the conformational changes attributable to the allosteric transition of the holoenzyme remain to be defined.

Crystallographic studies of allosteric proteins, such as hemoglobin (1), glycogen phosphorylase (2, 3), phosphofructokinase (4), and aspartate transcarbamoylase (5), in both unliganded and liganded conformations have provided invaluable structural information needed for interpreting their regulatory properties. Structural rearrangements in these proteins accompanying the binding of active-site ligands were demonstrated clearly. Nonetheless, crucial knowledge of the allosteric transitions is still lacking. How are the unliganded proteins converted from the low-affinity (or low-activity), taut, **T** conformation to the high-affinity (or high-activity), relaxed, **R** state? For many allosteric proteins, the **T** conformation dominates the equilibrium population of unliganded molecules. As a result, it has not been possible to determine structures of the unliganded proteins in the **R** state. In the absence of such information, the structures of the liganded allosteric proteins were assumed to represent the **R** conformation even though it is recognized that ligand binding can have localized structural effects in addition to the more global impact caused by allosteric activation.

Interest in the structure of the **R** conformation of *Escherichia coli* aspartate transcarbamoylase (ATCase; aspartate carbamoyltransferase, carbamoyl phosphate:L-aspartate carbamoyltransferase; EC 2.1.3.2) and its relationship to the structure of the complex of ATCase with the bound bisubstrate ligand *N*-phosphonacetyl-L-aspartate (PALA) was stimulated recently by the crystal structure of the highly active, nonallosteric, catalytic (C) subunit (6). The C trimer lacked threefold symmetry and exhibited greater overall flexibility and disorder in loops containing active-site residues. Most unexpectedly, the overall conformation of the C trimer resembled the trimers within the unliganded, relatively inactive, **T** state holoenzyme (6). This similarity to the unliganded holoenzyme (7) rather than to the PALA–ATCase complex (8), coupled with the flexibility of the isolated C trimer, led to the suggestion that activation of ATCase involves removal of constraint inherent in the unliganded holoenzyme (6).

In contrast, the PALA-liganded holoenzyme has been thought to represent the **R** state structure (5, 9). This assumption was based on the finding that substoichiometric amounts of PALA, like the presence of both substrates (10), led to marked activation of ATCase (11, 12). Moreover, the global conformational changes associated with activation are complete even upon partial occupancy of the active sites by PALA (13, 14). Lipscomb and his colleagues (5, 7–9, 15) showed that unliganded ATCase and the PALA-bound enzyme differ markedly in structure. The rearrangements in quaternary structure include a 12-Å increase in the separation between the two C trimers and a 15° rotation of the regulatory dimers about the twofold axes. Accompanying these alterations are large changes in the tertiary structure of the catalytic chains. PALA binding promotes an 8° closure of the hinge between the two domains of the chain and reorganization of two functionally important loops containing active-site residues. These crystallographic studies, however, provide no information indicating how much of the conformational change in ATCase accompanying PALA binding is attributable directly to the localized effects of the ligand and how much to the indirect, global effect represented by the swelling of the enzyme (13, 16).

Because of the cooperative binding of PALA to ATCase, enzyme molecules with partial occupancy of the six active sites are rare. In the absence of structural information about the unoccupied active sites in partially liganded ATCase or unliganded ATCase in the **R** state, the localized effects of PALA binding can be evaluated by studies on the free C trimer. Here we show that the C trimer–PALA complex structurally resembles the

---

Abbreviations: ATCase, aspartate transcarbamoylase; C, catalytic (subunit or trimer); PALA, *N*-(phosphonacetyl)-L-aspartate; **R**, relaxed, active; **T**, taut, inactive.

Data deposition: The atomic coordinates of C trimer–PALA have been deposited in the Protein Data Bank, www.rcsb.org (PDB ID code 1EKX).

*P.T.B. and J.A.E. contributed equally to this work.

†Present address: Molecular and Structural Biology Division, E. O. Lawrence Livermore National Laboratory, 7000 East Avenue L-448, Livermore, CA 94551.

‡To whom correspondence and reprint requests should be addressed at: Department of Molecular and Cell Biology, University of California, 229 Stanley Hall # 3206, Berkeley, CA 94720-3206. E-mail: schach@socrates.berkeley.edu.

The publication costs of this article were defrayed in part by page charge payment. This article must therefore be hereby marked "*advertisement*" in accordance with 18 U.S.C. §1734 solely to indicate this fact.

Article published online before print: *Proc. Natl. Acad. Sci. USA*, 10.1073/pnas.090087197. Article and publication date are at www.pnas.org/cgi/doi/10.1073/pnas.090087197

Table 1. Data collection and refinement statistics

Crystals	
Space group	$P2_12_12_1$
Unit cell dimensions, Å	a = 58.12, b = 82.13, c = 252.51
V_m, Å^3/Da	2.93
Data collection	
Resolution range, Å	20–1.95
Unique/measured reflections	86,079/125,472
Completeness, %	92.6 (81.1)
Average $I/\sigma I$	10.2 (3.3)
R_{merge}, %	7.8
Refinement	
R/R_{free}, %	17.1/21.4
Reflections in the free R set	4,136
rms deviations	
Bond lengths, Å	0.015
Bond angles, °	1.70
Planar groups, Å	0.010

Values in parentheses reflect the data in the 2.0–1.95 resolution shell.

PALA-liganded C subunits within the holoenzyme. These similarities indicate that much of the change observed in the holoenzyme upon PALA binding arises from localized effects of ligand binding. These results demonstrate that the conformational changes caused by the allosteric transition remain to be identified.

Experimental Procedures

Protein Purification and Crystallization. ATCase, containing a His_6 sequence at the N terminus of each regulatory chain, was purified as described (17). Wild-type C trimer was isolated from the His-tagged holoenzyme by treatment with neohydrin followed by chromatography (18). The purified C subunit (6), at 6.1 mg/ml, was cocrystallized with PALA at 4°C by vapor diffusion. Crystals grew from 5 μl of 0.1 M Tris·HCl at pH 6.8/0.02 M $Ca(OAc)_2$/5.8% PEG 8000 and 5 μl of C subunit in 10 mM Tris·HCl at pH 7.5/1 mM 2-mercaptoethanol/2 mM PALA. The crystals contained a single C trimer–PALA complex in the asymmetric unit.

Data Collection and Structure Determination. Crystals (0.50 × 0.10 × 0.05 mm) were equilibrated in 40 mM Tris·HCl at pH 6.8/20 mM $Ca(OAc)_2$/29% PEG 8000/22% methylpentanediol, mounted on a nylon loop, and flash cooled in liquid N_2. High-resolution (20–1.95 Å) data were collected at 100 K from a single crystal at Beamline 5.0.2 at the Lawrence Berkeley National Laboratory Advanced Light Source. The data were integrated with DENZO (19) and scaled by using SCALA (20).

Molecular replacement was performed by using AMoRe (21), with a threefold symmetric search model constructed from the structure of the ATCase–PALA complex (22) with the PALA removed. The rotation function yielded three peaks above 11σ related by 120° rotations. Each of these rotation function solutions yielded the same 16σ translation function solution. The molecular replacement solution had an initial R factor of 40.4%, which was reduced to 34.1% with rigid body refinement. The model was refined by iterative cycles of positional and B factor refinement using TNT (23) followed by model building with O (24). After the high symmetry of the C trimer–PALA complex became evident, noncrystallographic symmetry (ncs) restraints were applied with medium weights by using REFMAC (25). The ncs restraints were relaxed at the end of refinement. This procedure reduced the R_{free} value from 23.8% to 21.4% with a minimal change in R. The refined model contains 8,085 atoms, including 7,212 protein atoms (926/930 amino acids), 3 PALA molecules, 823 water molecules, and two Ca^{2+} atoms. All residues exhibit allowed main-chain dihedral angles. The crystallographic data are summarized in Table 1.

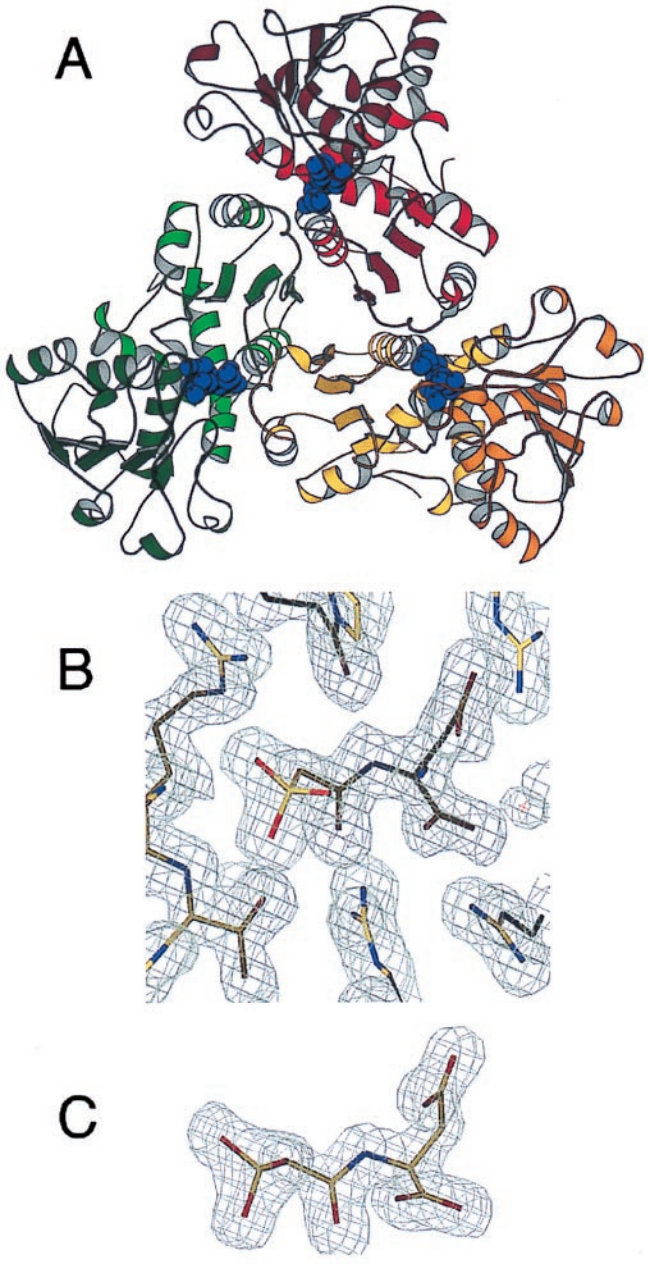

Fig. 1. Structure of the C trimer–PALA complex at 1.95-Å resolution. (*A*) Ribbon representation of the PALA-liganded C trimer. Each chain is shown in a different color with the N-terminal, carbamoyl-phosphate-binding domain (center), depicted in a lighter shade than the C-terminal, aspartate-binding, domain. PALA is shown in blue Corey–Pauling–Koltun rendering, highlighting both the interchain and interdomain location of the active sites. (*B*) $2F_o - F_c$ electron density map (contour level 1σ) in the region of the bound bisubstrate analog. (*C*) Omit $F_o - F_c$ map of the inhibitor, PALA (contour level 3σ), using phases calculated from a model excluding the PALA molecule.

Hinge Angle and Chain Comparisons. Differences in hinge angles were calculated, using GEM (26), as the angle required to reorient a superimposed pair of N-terminal domains to reach superposition of the attached C-terminal domains. Superpositions were

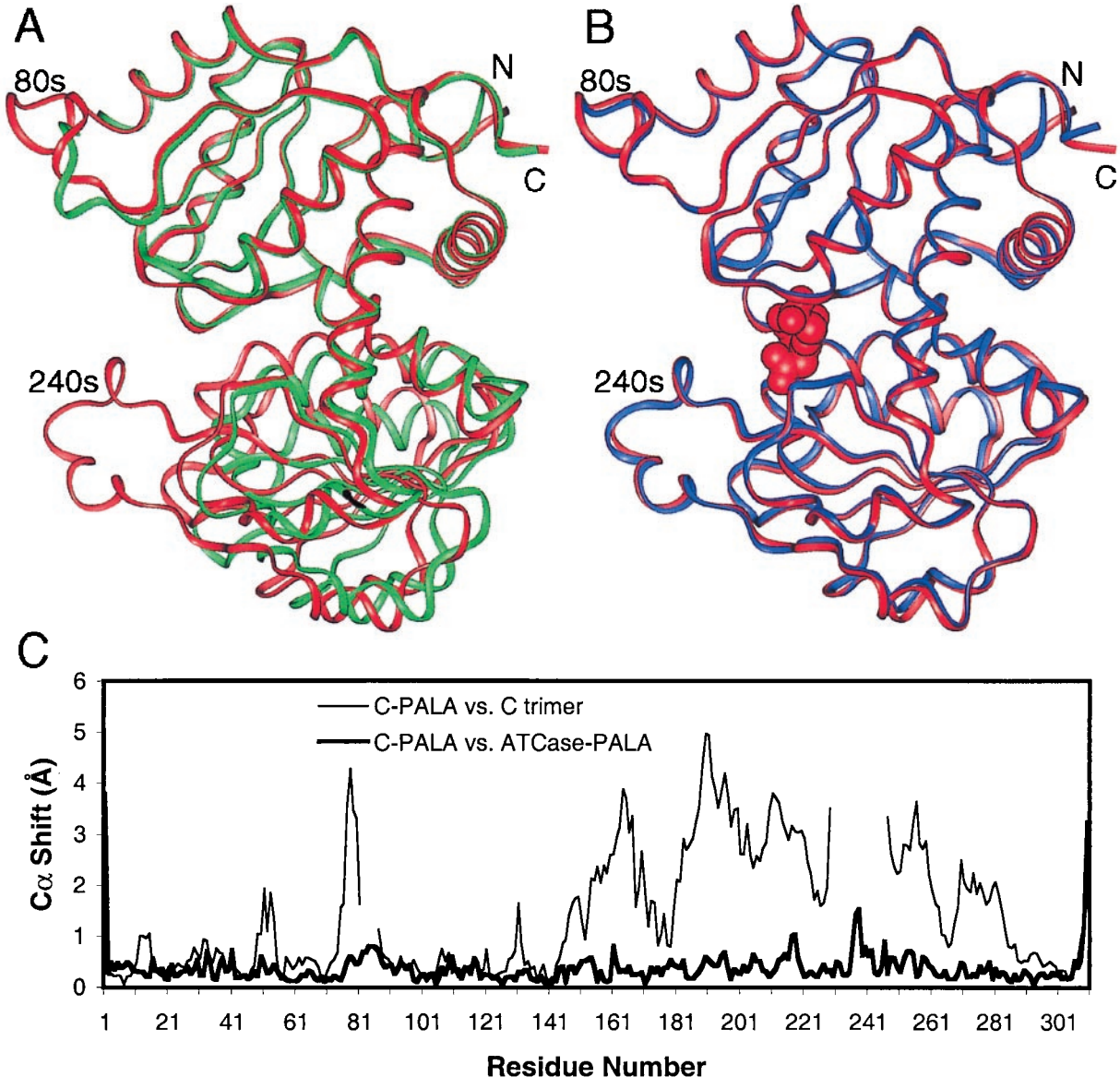

Fig. 2. The catalytic chains in the C trimer exhibit pronounced hinge closure upon PALA binding and adopt a conformation very similar to that of the chains in the PALA-bound holoenzyme. (*A*) Superposition of the N-terminal domains of catalytic chains from the C trimer–PALA complex (red) and the unliganded C trimer (PDB ID 3csu, Y chain, green). The chains superimpose closely within each domain but exhibit a 9.5° difference in hinge angle. (*B*) Superposition of catalytic chains from the C trimer–PALA complex (red) and the holoenzyme–PALA complex (PDB ID 1D09, blue). The similarity of the liganded conformations indicates that PALA binding is sufficient to promote the closed hinge in the holoenzyme. PALA is shown in red as a space-filling model. (*C*) Shift plots depicting differences in C^{α} positions as a function of residue number. Shift corresponding to *A* (chain from the C trimer–PALA complex versus the Y chain of the unliganded C trimer) is shown as a thin line illustrating a large relative motion of one domain with a hinge near Leu-140. Shift plot corresponding to *B* (chain from the C trimer–PALA complex versus a catalytic chain from the holoenzyme–PALA complex) is shown as a thick line. This comparison shows close similarity, except at the termini and the 240s loop.

performed with main-chain atoms of residues 1–73 and 90–134 for the N-terminal domain and residues 150–229 and 252–284 for the C-terminal domain. The interdomain helices and the 80s and 240s loops were excluded in the construction of the superimposed models. Backbone rms deviations and active site comparisons were based on superpositions of residues 5–305.

Results

Fig. 1*A* shows the structure of the C trimer–PALA complex, determined by molecular replacement using a trimeric search model derived from the structure of the holoenzyme–PALA complex (22) with the bisubstrate analog removed. The structure was refined to R and R_{free} values of 17.1% and 21.4%, respectively, using all of the data from 20–1.95 Å. The resulting $2F_o - F_c$ maps (Fig. 1*B*) revealed continuous electron density for 926/930 residues, 823 H_2O molecules, and 2 Ca^{2+} ions. Omit maps (Fig. 1*C*) confirm the presence of the bisubstrate analog in all three active sites.

In contrast to the unliganded C trimer, the PALA complex exhibits almost complete threefold symmetry. Hinge angles between the N- and C-terminal domains in each of the three PALA-liganded chains differ by less than 1.3°. The rms deviations for backbone atoms are small (0.26–0.34 Å). Both the 80s and 240s loops adopt specific, approximately symmetric conformations (Fig. 2*A*).

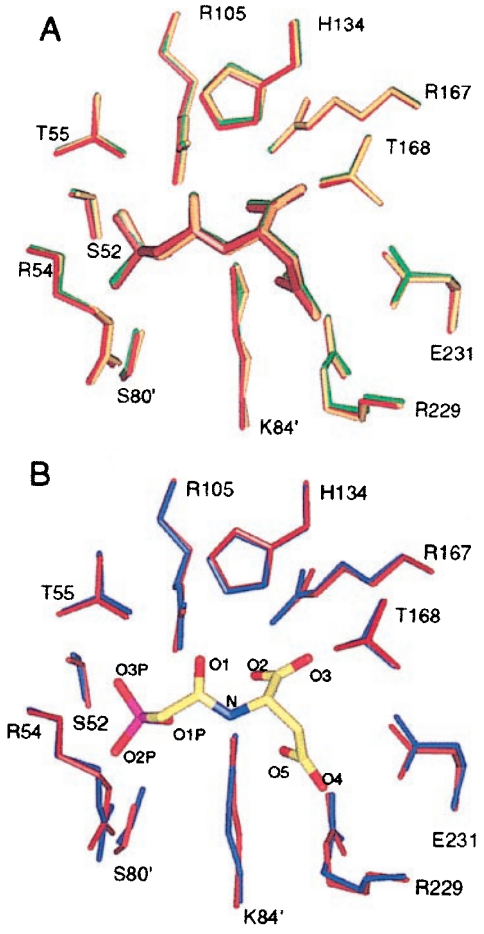

Fig. 3. Similar active-site conformations in PALA-liganded C trimer and holoenzyme. (*A*) Comparison of the three active sites in the C trimer–PALA complex, based on the superposition of all backbone atoms, shows nearly identical conformations. (*B*) Comparison of an active site in the C trimer–PALA complex (red) with that in the holoenzyme–PALA complex (blue). The conformation of PALA is very similar in both structures and is shown for only the C trimer–PALA complex. Slight differences are observed in rotamers of Arg-54.

Inhibitor contacts in the C trimer–PALA complex were very similar to those in the holoenzyme-PALA complex. The enzyme surrounds the bisubstrate inhibitor, and contacts are formed with every polar atom in PALA (Fig. 3). All three PALA molecules have similar contacts with active-site residues and form hydrogen bonds to three buried solvent molecules. The carboxylates of PALA complement positively charged residues, Arg-105, Arg-229, and Lys-84′ (where ′ denotes a residue from an adjacent chain), and the PALA phosphonate contacts Arg-105 and Arg-54.

The bound PALA also forms intramolecular contacts between atoms O1 and O2 (2.9 Å), O3P and O1 (3.2 Å), and between O1P and O2 (3.5 Å). The two carboxylates of the inhibitor are in a nearly eclipsed conformation. A solvent molecule bridges the carboxylates between O2 and O5. The high-resolution structure of the C trimer–PALA complex reveals the locations of many bound solvent molecules. In addition to the water molecules bound at the active sites, buried water molecules are distributed throughout the structure, including the "tunnel" along the pseudo-threefold axis of the trimer. Notably, the 240s loop packs with water molecules interposing between main-chain atoms of the loop and the remainder of the C-terminal domain.

Discussion

Conformational Changes in C Trimer Resulting from PALA Binding. Liganded C trimer (Fig. 1*A*) exhibits approximate threefold symmetry. In contrast, the unliganded C trimer is much more asymmetric, with a larger variation (4.8°) in interdomain hinge angles and variable conformations of the 80s and 240s loops (6). The large conformational change accompanying the binding of PALA (Fig. 2 *A* and *C*; Table 2) involves substantial closure (7.7–13.2°) of the hinge between the N- and C-terminal domains. The range in hinge angle differences is primarily due to the asymmetry observed for the unliganded C trimer, for which the hinge angles of the three chains in the crystallographic asymmetric unit vary as much as 4.8° (6).

In addition to the large reduction in hinge angles, PALA binding results in significant alterations in the local backbone conformation of residues in the binding site. These changes affect the phosphate-binding loop (residues 52–55), as well as the 80s and 240s loops. In the unliganded C trimer, the loops are disordered, as judged by the weak electron density, high *B* values, and large conformational differences among the three chains (6). PALA binding to the C trimer is accompanied by ordering of the 80s and 240s loops and large changes in the vicinity of residues Ser-52, Ser-80, and Arg-229, which make inhibitor contacts. Additional significant differences (>1.5 Å) in local main chain conformations were apparent in superpositions of the N- and C-terminal domains (Fig. 2*C* and data not shown). Residues Ile-12, Ser-80, Glu-204, and Arg-229, which display 2- to 4-Å backbone shifts, are near sites that interact with the regulatory chains in the holoenzyme. These shifts, as well as changes in the active-site loops, presumably are associated with formation of the dodecamer–bisubstrate complex. As a result, they identify potential communication pathways between the active sites and the regulatory sites. Shifts in surface residues Arg-183, Glu-204,

Table 2. Variations in catalytic chain hinge angles

	ATCase* (unliganded)	ATCase–PALA†	C trimer chain X	C trimer chain Y	C trimer chain Z
ATCase–PALA	7.5–8.6	—	—	—	—
C trimer chain X	−(5.6–6.0)	−12.5	—	—	—
C trimer chain Y	−(3.6–3.7)	−9.4	3.7	—	—
C trimer chain Z	−(1.1–1.3)	−8.5	4.8	2.5	—
C trimer–PALA	7.0–8.7	−(0.6–1.6)	11.3–13.2	9.1–9.5	7.7–8.6

A positive hinge-angle difference (in degrees) corresponds to a more open hinge in the structure listed at the top of each column. Hinge angles were calculated as described in *Experimental Procedures.* Ranges are given for comparisons involving at least one structure with multiple conformations that differ by >0.3°.

*Calculated with catalytic chains from the coordinates of Ke *et al.* (27). The two catalytic chains in the asymmetric unit differ in hinge angle by 1.0°.

†Calculated with catalytic chains from the coordinates of the ATCase–PALA complex (8). The two catalytic chains in the asymmetric unit differ in hinge angle by 0.3°.

Val-218, Phe-247, and Gln-297 may reflect the influence of nearby contacts between molecules in the crystal lattice. Thus, most of the large local differences between the free and PALA-bound C trimers are associated with variations in crystal packing or with ligand interactions.

Comparison of PALA-Liganded C Trimer and Liganded Holoenzyme. The approximate threefold symmetry of the C trimer–PALA complex is similar to the exact crystallographic threefold symmetry observed for both the unliganded (27) and liganded (8) holoenzymes. Whereas the hinge angles of the catalytic chains in the C trimer–PALA complex are 7.0–8.7° more closed than in the chains of the unliganded holoenzyme, they differ only slightly (0.6–1.6°) from those of PALA-bound ATCase (Fig. 2 *B* and *C*; Table 2). It is significant that the differences in hinge angles among the chains in the PALA-liganded C trimer ($\approx$1.2 Å) are larger than the variations ($<$0.3°) in the holoenzyme–PALA complex. Thus, the high degree of symmetry in the holoenzyme is partially attributable to assembly of the dodecamer from two C trimers and three regulatory dimers.

The tertiary structures of the catalytic chains in the C trimer–PALA complex are similar to one another and to those in the PALA-liganded holoenzyme (Fig. 2 *B* and *C*). Small rms deviations (0.39–0.44 Å) are evident for backbone atoms in the liganded trimer versus the holoenzyme–PALA complex (8). The 80s and 240s loops, which interact directly with PALA, adopt equivalent conformations in the two liganded structures. The positions of PALA and most active-site residues are nearly identical in superpositions of entire chains (Fig. 3).

PALA adopts the same conformation and makes virtually identical contacts to the active-site residues in the complexes of the C trimer and the holoenzyme (Fig. 3*B*). Compared with the holoenzyme–PALA complex at 2.5-Å resolution (22), which was used as a molecular replacement model, several differences in active-site rotamers were observed and were attributed to the higher resolution of the C trimer rather than real structural differences. The recently described structure (8) of the holoenzyme–PALA complex at 2.1-Å resolution has revised rotamers for Arg-229 relative to the earlier version, and these are consistent with the rotamer assignments in the C trimer–PALA complex (Fig. 3*B*). The C trimer–PALA complex also differed from the 2.5-Å structure of the holoenzyme–PALA complex in the conformation of Arg-54, a residue that binds the PALA phosphonate group. The rotamer observed in all three catalytic chains in the C trimer–PALA complex makes two hydrogen bonds with the phosphonate O2P, versus one in the previously described holoenzyme complex (22). Interestingly, the high-resolution structure of the holoenzyme-PALA complex has one Arg-54 modeled in each of the two conformations (8). No contextual basis is apparent for the differences in Arg-54 rotamer assignments in the holoenzyme complex. In the C trimer–PALA complex, His-134, which lies adjacent to the N terminus of a helical turn, is hydrogen bonded to a buried water molecule, which was not detected in the structure of the ATCase–PALA complex.

The only backbone difference $>$2 Å is near Glu-239, which mediates contact between the two C trimers in the unliganded holoenzyme and forms an intrachain hydrogen bond when PALA is bound. Smaller differences are observed near Leu-38 and Ser-80, which contribute to interchain contacts within a C trimer, and Glu-204, which interacts with a regulatory chain. Residues in the region of Leu-38 and Glu-204 also contribute to crystal contacts. Thus, some of the significant differences in the local backbone conformation of the PALA complexes of the C trimer and the holoenzyme may be attributable to crystal contacts that differ in the two crystal environments.

Implications for the Allosteric Mechanism of ATCase. The allosteric transition of ATCase has been defined largely in terms of the interconversion of the unliganded holoenzyme representing the **T** state (27, 28) and the conformation observed in the ATCase–PALA complex (8, 15). These structures differ not only in their global conformations, represented by the separation of the two C trimers and the orientation of the three regulatory dimers, but also in the tertiary structures of the 12 polypeptide chains. In particular, the hinges connecting the N- and C-terminal domains of the catalytic chains close and active site loops undergo large changes upon PALA binding. Whether these conformational changes result from the binding event or occur as an indirect effect of the allosteric transition is not known. Nor is there information relevant to the linkage between the alterations in quaternary structure and the changes in the tertiary structures of the individual chains. Can the separation of the two C trimers in the holoenzyme be increased by 12 Å, for example, without the concomitant closure of the hinge between the two domains? Conversely, can the hinges close without an increased separation of the two trimers? These questions cannot be answered through studies on wild-type ATCase, which exists predominantly in the compact **T** state conformation in the absence of active-site ligands (29). Answering these questions requires a determination of the structure of the unliganded, activated holoenzyme in the relaxed, **R** state. In the absence of such structural information we have characterized the highly active, isolated, nonallosteric C trimer to determine the effect of the binding of the bisubstrate ligand.

Assembly of the holoenzyme in the **T** state involves a decrease in flexibility and only small changes in the average structure of the catalytic chains (6). Flexibility in the unliganded C trimer is indicated by differences among the catalytic chains, including hinge angles that vary up to 4.8°. The hinges are more open than those in the **T** state holoenzyme and much more open than those in the ATCase–PALA complex (6). The high activity of the C trimer, coupled with its structural similarity to the much less active **T** state holoenzyme, led to the suggestion that activation of ATCase involves the release of constraints that impair catalytic activity (6). This concept of deconstraint, also invoked for other enzymes (30–33), led us to question the generally accepted view that the ATCase–PALA structure represents the **R** state.

This hypothesis is supported by the evidence presented here showing that PALA-bound C trimers adopt similar conformations in isolation and in the ATCase holoenzyme (Fig. 2*B*; Table 2). The liganded chains in the C trimer have hinge angles and tertiary structures virtually identical to those in the ATCase–PALA complex (Figs. 2 and 3; Table 2). Binding of PALA to the C trimer is clearly sufficient to produce the closed hinge conformation. Although direct evidence is lacking, it is plausible to assume that the closure of the hinges in the holoenzyme also is attributable to the direct effect of PALA binding and that the alterations in the tertiary structure of the catalytic chains do not define the global conformational change associated with the allosteric transition. Conversely, there is no *a priori* basis for concluding that the allosteric transition would result in such pronounced hinge closure in the absence of the bisubstrate ligand. Indeed, the openness of the hinges in the unliganded C trimer supports the view that access of the substrates to the active sites requires open hinges and that closure before aspartate binding would inhibit the enzyme. It is worth noting that analysis of the kinetics of the interaction of PALA with the C trimer, using a variety of techniques (34), led to a mechanism involving a rapid binding of the bisubstrate ligand followed by a much slower isomerization of the complex. When carbamoyl phosphate and aspartate are added to a solution containing the C trimer–PALA complex there is a substantial lag in catalytic activity before the linear formation of carbamoyl aspartate. This lag, which is readily interpreted in terms of a reverse isomerization of the complex, could be represented by the slow opening

of the hinge required for release of PALA and access by the substrates.

Studies of the holoenzyme by UV absorption spectroscopy revealed distinct structural alterations caused by the binding of PALA, on the one hand, and the global conformational change on the other (35). Similarly, calorimetric studies showed distinct enthalpy changes resulting from the allosteric transition and PALA binding (36). These studies support the conclusion that the structure of the PALA-liganded holoenzyme differs from the activated (**R**) state of ATCase.

As an analog of the true bisubstrate complex, however, the ATCase–PALA structure defines a catalytic intermediate that must be accessible in the activated **R** state. The large variations in structures of the free and liganded holoenzyme indicate that substantial conformational changes accompany turnover. Consequently, activated ATCase must be capable of traversing diverse productive conformations, one of which resembles the PALA complex. Establishing the linkage between the global, allosteric transition and the local conformational effects of PALA binding requires additional structural information.

This research was supported by National Institutes of Health/National Institute of General Medical Sciences Research Grant GM 12159 to H.K.S., Research Grant GM 54793 to T.A., and National Research Service Award 19014 to P.T.B. The Advanced Light Source is supported by the Director, Office of Science, Office of Basic Energy Sciences, Materials Sciences Division, of the U.S. Department of Energy under Contract DE-AC03–76SF00098 at Lawrence Berkeley National Laboratory.

1. Perutz, M. F. (1989) *Q. Rev. Biophys.* **22,** 139–236.
2. Fletterick, R. J. & Sprang, S. R. (1982) *Acc. Chem. Res.* **15,** 361–369.
3. Johnson, L. & Barford, D. (1990) *J. Biol. Chem.* **265,** 2409–2412.
4. Schirmer, T. & Evans, P. (1990) *Nature (London)* **343,** 140–145.
5. Lipscomb, W. N. (1994) *Adv. Enzymol.* **68,** 67–151.
6. Beernink, P. T., Endrizzi, J. A., Alber, T. & Schachman, H. K. (1999) *Proc. Natl. Acad. Sci. USA* **96,** 5388–5393.
7. Stevens, R. C., Gouaux, J. E. & Lipscomb, W. N. (1990) *Biochemistry* **29,** 7691–7701.
8. Jin, L., Stec, B., Lipscomb, W. N. & Kantrowitz, E. R. (1999) *Proteins* **37,** 729–742.
9. Stevens, R. C., Chook, Y. M., Cho, C. Y., Lipscomb, W. N. & Kantrowitz, E. R. (1991) *Protein Eng.* **4,** 391–408.
10. Gerhart, J. C. & Pardee, A. B. (1962) *J. Biol. Chem.* **237,** 891–896.
11. Collins, K. D. & Stark, G. R. (1971) *J. Biol. Chem.* **246,** 6599–6605.
12. Foote, J. & Schachman, H. K. (1985) *J. Mol. Biol.* **186,** 175–184.
13. Howlett, G. J. & Schachman, H. K. (1977) *Biochemistry* **16,** 5077–5083.
14. Blackburn, M. N. & Schachman, H. K. (1977) *Biochemistry* **16,** 5084–5091.
15. Ke, H., Lipscomb, W. N., Cho, Y. & Honzatko, R. B. (1988) *J. Mol. Biol.* **204,** 725–747.
16. Gerhart, J. C. & Schachman, H. K. (1968) *Biochemistry* **7,** 538–552.
17. Graf, R. & Schachman, H. K. (1996) *Proc. Natl. Acad. Sci. USA* **93,** 11591–11596.
18. Yang, Y. R., Kirschner, M. W. & Schachman, H. K. (1978) *Methods Enzymol.* **51,** 35–41.
19. Otwinowski, Z. & Minor, W. (1996) *Methods Enzymol.* **276,** 307–326.
20. Collaborative Computational Project Number 4 (1994) *Acta Crystallogr. D* **50,** 760–763.
21. Navaza, J. (1994) *Acta Crystallogr. A* **50,** 157–163.
22. Krause, K. L., Volz, K. W. & Lipscomb, W. N. (1987) *J. Mol. Biol.* **193,** 527–553.
23. Tronrud, D. E., Ten Eyck, L. F. & Matthews, B. W. (1987) *Acta Crystallogr. A* **43,** 489–501.
24. Jones, T. A., Zou, J. Y., Cowan, S. W. & Kjeldgaard, M. (1991) *Acta Crystallogr. A* **47,** 110–119.
25. Murshudov, G., Vagin, A. & Dodson, E. (1997) *Acta Crystallogr. D* **53,** 240–255.
26. Fauman, E. B., Rutenber, E. E., Maley, F. & Stroud, R. M. (1994) *Biochemistry* **33,** 1502–1511.
27. Ke, H.-M., Honzatko, R. B. & Lipscomb, W. N. (1984) *Proc. Natl. Acad. Sci. USA* **81,** 4037–4040.
28. Kim, K. H., Pan, Z., Honzatko, R. B., Ke, H.-M. & Lipscomb, W. N. (1987) *J. Mol. Biol.* **196,** 853–875.
29. Howlett, G. J., Blackburn, M. N., Compton, J. G. & Schachman, H. K. (1977) *Biochemistry* **16,** 5091–5099.
30. Monod, J., Wyman, J. & Changeux, J.-P. (1965) *J. Mol. Biol.* **12,** 88–118.
31. Schuller, D., Grant, G. & Banaszak, L. (1995) *Nat. Struct. Biol.* **2,** 69–76.
32. Buchbinder, J. & Fletterick, R. (1996) *J. Biol. Chem.* **271,** 22305–22309.
33. Xu, W., Doshi, A., Lei, M., Eck, M. & Harrison, S. (1999) *Mol. Cell* **3,** 629–638.
34. Cohen, R. E. & Schachman, H. K. (1986) *J. Biol. Chem.* **261,** 2623–2631.
35. Hu, C. Y., Howlett, G. J. & Schachman, H. K. (1981) *J. Biol. Chem.* **256,** 4998–5004.
36. Shrake, A., Ginsburg, A. & Schachman, H. K. (1981) *J. Biol. Chem.* **256,** 5005–5015.